AIP Applied Physics Letters

50 50 beam splitter using a one-dimensional metal photonic crystal with parabolalike dispersion

Linfang Shen, Tzong-Jer Yang, and Yuan-Fong Chau

Citation: Applied Physics Letters **90**, 251909 (2007); doi: 10.1063/1.2750385
View online: http://dx.doi.org/10.1063/1.2750385
View Table of Contents: http://scitation.aip.org/content/aip/journal/apl/90/25?ver=pdfcov
Published by the AIP Publishing

50/50 beam splitter using a one-dimensional metal photonic crystal with parabolalike dispersion

Linfang Shen[a)]
Department of Information Science and Electronic Engineering, Electromagnetic Academy, Zhejiang University, Hangzhou 310027, China

Tzong-Jer Yang
Department of Electrophysics, National Chiao Tung University, Hsinchu, 30050 Taiwan, Republic of China

Yuan-Fong Chau
Department of Electronic Engineering, Chin Yun University, Jung Li, 320 Taiwan, Republic of China

(Received 12 October 2006; accepted 26 May 2007; published online 19 June 2007)

The spatial dispersion properties of a one-dimensional metal photonic crystal have been analyzed and five types of dispersion curves have been shown at a normalized frequency less than 1. It is demonstrated that by exploiting a parabolalike dispersion behavior, a metal photonic crystal slab can be used to realize an exactly 50/50 beam splitter.
[DOI: 10.1063/1.2750385]

The dispersion characteristics of photonic crystals (PCs) have recently attracted considerable interest. Various spatial dispersion properties of PCs underlay foundation for a variety of potential applications such as spatial beam routing[1] and dispersion-based beam splitter.[2,3] So far, the known studies of the spatial dispersion phenomena of PCs are mainly devoted to dielectrics PCs (DPCs),[4–6] while very few refer to metal PCs (MPCs).[7,8] This can be explained by the fact that metals in the visible/infrared range are often accompanied by absorption loss, which creates an obvious obstacle in utilizing MPCs in practical devices. However, if the filling fraction of metallic material in the MPC is small enough, it is possible to reduce the influence of absorption loss to a tolerable level. Compared to DPCs, MPCs comprised of materials with permittivities of opposite signs provide more opportunities of exhibiting unusual dispersion behaviors. We also notice some recent research works on PCs containing left-handed materials that have simultaneously negative permittivity and permeability.[9–11] In this letter, we will study the dispersion characteristic of a one-dimensional (1D) MPC with a small metal filling fraction and demonstrate a MPC slab with special dispersion property to realize a 50/50 beam splitter.

Consider a 1D MPC consisting of silver films and SiO_2 layers stacked alternatively with a period a along the x direction. The silver films have a thickness $d \ll a$, i.e., its filling fraction $f_m = d/a \ll 1$. The interaction of an electromagnetic wave inside such MPC with the structure can be effectively interpreted through a dispersion diagram. For TE-polarized waves (with the magnetic field in the y direction) propagating in the xz plane ($\mathbf{k} = \hat{x}k_x + \hat{z}k_z$), the dispersion relation is given by

$$\cos(k_x a) = \cos[(1-f_m)p_x a]\cosh(f_m q_x a) - \frac{1}{2}\left(\frac{\varepsilon_m p_x}{\varepsilon_r q_x} - \frac{\varepsilon_r q_x}{\varepsilon_m p_x}\right) \times \sin[(1-f_m)p_x a]\sinh(f_m q_x a), \quad (1)$$

where ε_m and ε_r are the relative permittivities of silver and SiO_2, respectively; $p_x = \sqrt{\varepsilon_r k_0^2 - k_z^2}$ and $q_x = \sqrt{k_z^2 - \varepsilon_m k_0^2}$ with $k_0 = \omega/c$, where ω is the angular frequency of the wave and c the speed of light in free space. Here, we take $\varepsilon_r = 2.1$, while the dispersive ε_m is taken from Ref. 12. k_x is limited to the first Brillouin zone, i.e., $-\pi/a \leq k_x \leq \pi/a$.

To distinguish propagating waves from evanescent waves in the MPC and find the dispersion properties of the structure, we first neglect the imaginary part of ε_m in Eq. (1). To illustrate typical dispersion behaviors, the dispersion curves, namely, the equifrequency contours, for a MPC with a filling fraction of $f_m = 0.07$ at a normalized frequency of $\omega a/2\pi c = 1/3$ are shown in Fig. 1. Since ε_m is frequency dependent, the dispersion properties of such a PC cannot be characterized simply by the normalized frequency. Thus, as seen from Fig. 1, there exist five types of shapes of dispersion curves at the same normalized frequency for this PC. Here we choose a fixed normalized frequency ($\omega a/2\pi c = 1/3$) only to ensure that no higher-order Bragg coupling occurs in our subsequent application of this MPC.[6] The corresponding wavelengths of waves in free space ($\lambda = \omega/2\pi c$) in the five cases are 1.94, 1.24, 0.76, 0.66, and 0.41 μm, and

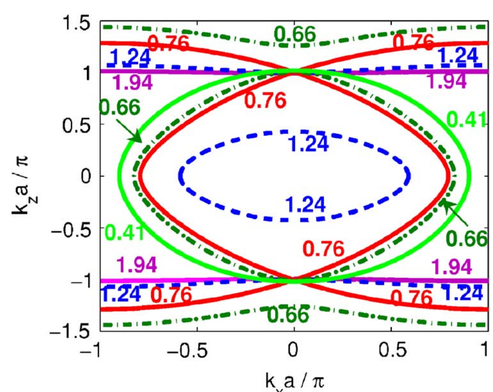

FIG. 1. (Color online) Dispersion curves for TE waves at various wavelengths for MPCs with a filling fraction $f_m = 0.07$. Normalized frequency $\omega a/2\pi c$ is 1/3 for all cases. The numbers marked indicate the values of wavelengths.

a)Electronic mail: lfshen@zju.edu.cn

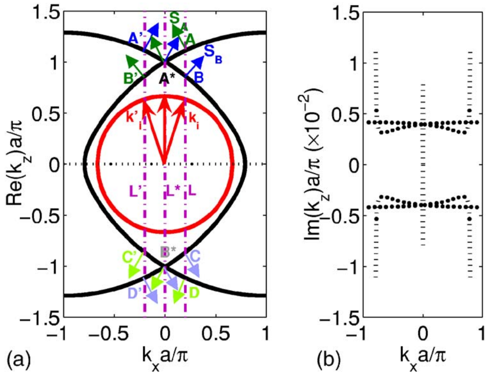

FIG. 2. (Color online) Wave vector diagram (for TE waves) for a MPC with f_m=0.07 and ε_m=−27.5+0.3i. (a) Re(k_z), (b) Im(k_z). The red circle in (a) is the equifrequency contour for air, and the dotted line indicates the direction of the interface between the MPC and air. The dot-dashed lines are the construction lines for three cases of wave incidence from air. $\mathbf{k}_i$ and $\mathbf{k}'_i$ are symmetric about the line k_x=0, so are the intersections A (B) and A' (B'). The Poynting vectors of refracted waves are indicated by bold plain arrows. Note that $k_0a/\pi=2/3$.

the respective MPC periods are 0.65, 0.41, 0.25, 0.22, and 0.14 μm, respectively. The four types of the dispersion curves for the wavelengths λ=1.94, 1.24, 0.66, and 0.41 μm (corresponding to the silver permittivities ε_m=−198.2, −78, −20.1, and −5.2, respectively[12]) are similar to those found for the TM wave in a structure formed by a periodic array of uniaxial magnetic resonant scatters:[13] They are hyperbolalike curve, ellipselike curve, or hyperbolalike (ellipselike) curve combined with ellipselike (hyperbolalike) curve which passes through the vicinities of $k_z=\pm\sqrt{\varepsilon_r}k_0$ at k_x=0. However, of particular interest is the fifth type of the dispersion curves corresponding to the wavelength of 0.76 μm (i.e., ε_m=−27.5), the two branches of the dispersion curves cross at k_x=0, for which $k_z\approx\pm\sqrt{\varepsilon_r+f_m^2(\varepsilon_r-\varepsilon_m)/2}k_0$. Though this MPC cannot be approximated by an effectively homogeneous medium, we may use the quantities of the effective permittivities, which are defined by $\varepsilon_t=f_m\varepsilon_m+(1-f_m)\varepsilon_r$ and $\varepsilon_n=\varepsilon_m\varepsilon_r/[f_m\varepsilon_r+(1-f_m)\varepsilon_m]$,[14] instead of the parameters ε_m and f_m, to characterize the structure, and we find that the special dispersion behavior occurs at $\varepsilon_t\approx 0$, which never happens in a DPC. Note that the parameter $\varepsilon_n\approx\varepsilon_r$ for all cases since $f_m\ll 1$.

When $|\varepsilon_t|$ is much less than ε_r and $|\varepsilon_m|$, in the limiting case of $k_0a\ll 1$ and $|\mathbf{k}|a\ll 1$, the dispersion equation [Eq. (1)] reduces to

$$k_x^2=\left[\varepsilon_t+\frac{1}{12}(1-f_m)^2\varepsilon_r^2\left(k_0^2-\frac{k_z^2}{\varepsilon_n}\right)a^2\right]\left(k_0^2-\frac{k_z^2}{\varepsilon_n}\right). \qquad (2)$$

When ε_t=0, the dispersion curve becomes a pair of parabolas, i.e., $k_x=\pm(1-f_m)\varepsilon_r(k_0^2-k_z^2/\varepsilon_n)a/2\sqrt{3}$. Note that $f_m=\varepsilon_r/(\varepsilon_r-\varepsilon_m)$ in this case. So the special dispersion curves for the aforementioned MPC should be parabolalike. By taking appropriate filling fraction at each wavelength such that ε_t=0, our numerical analysis indicates that the parabolalike dispersion behavior is preserved, at least for the case of $\omega a/2\pi c\leq 0.5$. In what follows, we focus on the case of f_m=0.07 and λ=0.76 μm, as a typical example, to demonstrate that such a MPC with parabolalike dispersion has the potential of application in beam splitting.

The accurate dispersion diagram for a MPC with f_m =0.07 at λ=0.76 μm is shown in Fig. 2, where $a/\lambda=1/3$ and the silver loss is taken into account, ε_m=−27.5+0.3i.[12] For a given real k_x, k_z now becomes a complex number. However, the imaginary part of k_z (for propagating waves) is much less than the real part (see Fig. 2), indicating that propagating waves attenuate slowly in the MPC. Consider a plane wave incident from air with wave vector $\mathbf{k}_i$ on a boundary of such a MPC along the x direction (i.e., the periodic direction). Two Bloch waves corresponding to the wave vector points A and B will be excited inside the MPC,[4] as illustrated in Fig. 2(a). The Poynting vectors of the two Bloch waves $\mathbf{S}_A$ and $\mathbf{S}_B$, which point away from the source, are opposite in the x direction, indicating that one wave is negatively refracted and the other positively refracted. Interestingly, as $k_x=\mathbf{k}_i\cdot\hat{x}\to 0$ (i.e., approaching to the case of normal incidence), the wave vector points A and B fall onto the same point A^*, but the Poynting vectors $\mathbf{S}_A$ and $\mathbf{S}_B$ will not become identical, and they only tend to be symmetric with respect to the surface normal [see Fig. 2(a)], implying the existence of two different (but symmetric) refracted waves in the MPC. The reasoning behind this is the symmetry of the crossing dispersion curves with respect to the line k_x=0 which is normal to the boundary, as illustrated in Fig. 2(a). Evidently, for a normally incident Gaussian beam with a certain width, which has a finite symmetric angle span around its propagation direction, i.e., the direction of the surface normal, two symmetric beams, one in each side of the surface normal, will be excited inside the MPC due to the symmetry of the dispersion curves. The spatial separation of the two beams in the MPC will increase as they propagate away from the interface, so a MPC slab with a certain width can realize an exactly 50/50 beam splitter.

To verify the beam splitting behavior in the MPC, we simulate a Gaussian beam of width 5λ incident normally on a MPC slab with a thickness of w=10λ in both the lossy (ε_m=−27.5+0.3i) and lossless (ε_m=−27.5) cases, using the finite-difference time-domain technique with uniaxial perfectly matched layers.[15] The distribution of the amplitude of the magnetic field (H_y) (obtained by a Fourier transform for the given frequency) for the lossless case is shown in Fig. 3(a) and the field pattern for the lossy case is found to be similar. As seen from Fig. 3(a), the incident beam is split symmetrically when it enters the MPC slab between z=0 and z=10λ, and the split beams separate by nearly 12λ at the exit surface. Both output beams are parallel to the incident beam, which follows directly from the conservation of k_x across the interfaces for each plane wave component of the beam. Since $\omega a/2\pi c=1/3<0.5$,[6] no higher-order Bragg propagating beams exit from this MPC slab. Our numerical analysis shows that the output beams have approximately the same width as the incident beam. The total power of both output beams is nearly 60% (with respect to the incident power) in the lossless case, but it reduces to 40% in the lossy case.

Figure 3(b) shows the total power of the output beams as a function of the thickness of the MPC slab, where the lines with open and solid circles represent the results for the lossless and lossy cases, respectively. While the spatial separation of the exit beams increases linearly with the thickness w, the total output power varies almost periodically in both cases, as seen from Fig. 3(b), where a slow decaying of power peaks is also observed for the lossy case. The maximum of total output power is found to be 42% in the lossy case, whereas up to nearly 80% in the lossless case.

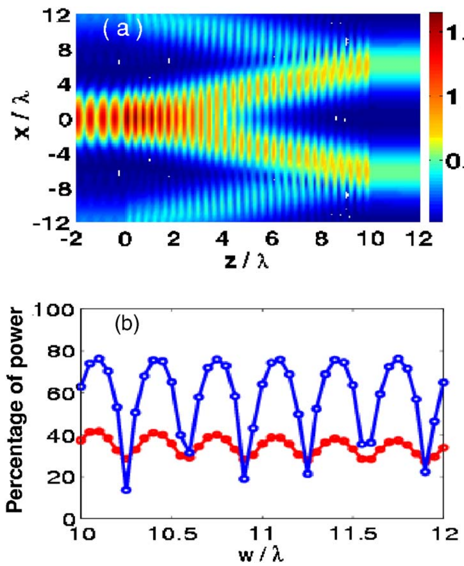

FIG. 3. (Color online) (a) Magnetic-field distribution for a TE-polarized Gaussian beam normally incident on a MPC slab with parabolalike dispersion. (b) Percentage of total output power versus the slab thickness w. The line with solid (open) circles corresponds to the lossy (lossless) case.

The MPC splitter can also output asymmetrically split beams as long as a Gaussian beam is incident obliquely on the MPC slab. For example, when a Gaussian beam of width 5λ is incident on the MPC slab with $w=10\lambda$ at an incidence angle of 30°, the output beams at the exit surface are shifted asymmetrically in the positive or negative x directions, but they are still parallel to the incident beam (see Fig. 4). The power ratio of the output beams is 1.7 and the total output power is 25% in the lossy case, while they become 2.2 and 60% in the lossless case, respectively. From Fig. 2(a), it seems evidently that the asymmetry of two split beams enhances with the increase of incidence angle.

To summarize, we have shown five types of dispersion curves for a 1D MPC at a normalized frequency less than 1. Among these, a parabolalike dispersion behavior has been found for the first time in PCs. By exploiting this special dispersion property, a MPC slab can be used to realize an exactly 50/50 beam splitter by normal incidence. Asymmetric beams with different output powers can also be obtained

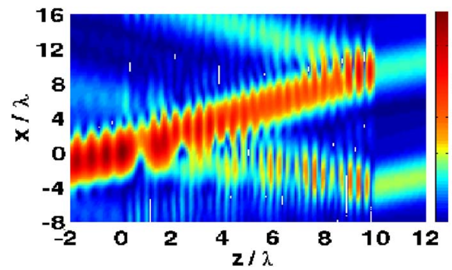

FIG. 4. (Color online) Magnetic-field distribution for a TE-polarized Gaussian beam incident on a MPC slab with $f_m=0.07$ and $\varepsilon_m=-27.5+0.3i$ at an incidence angle of 30°.

in a MPC splitter by oblique incidence. This MPC splitter works only for TE-polarized waves. Based on a similar mechanism, however, a splitter for TM-polarized waves can also be realized by using a photonic crystal formed by an array of magnetic resonant components such as nanowire pairs.

The authors would like to acknowledge the National Science Council of ROC for the financial support through the Grant the NSC 95-2119-M-009-029. One of the authors (L.S.) sincerely thanks the hospitality of NCTU when he visited there.

[1]D. W. Prather, S. Shi, D. Pustai, C. Chen, S. Venkataraman, A. Sharkawy, G. Schneider, and J. Murakowski, Opt. Lett. **29**, 50 (2004).
[2]X. Yu and S. Fan, Appl. Phys. Lett. **83**, 3251 (2003).
[3]S. Shi, A. Sharkawy, C. Chen, D. Pustai, and D. W. Prather, Opt. Lett. **29**, 617 (2004).
[4]P. St. J. Russell, Appl. Phys. B: Photophys. Laser Chem. **39**, 231 (1986).
[5]M. Notomi, Phys. Rev. B **62**, 10696 (2000).
[6]S. Foteinopoulou and C. M. Soukoulis, Phys. Rev. B **72**, 165112 (2005).
[7]X. Y. Ao and S. He, Opt. Lett. **30**, 2152 (2005).
[8]X. Fan, G. P. Wang, J. C. Lee, and C. T. Chan, Phys. Rev. Lett. **97**, 073901 (2006).
[9]J. Li, L. Zhou, C. T. Chan, and P. Sheng, Phys. Rev. Lett. **90**, 083901 (2003).
[10]H. Daninthe, S. Foteinopoulou, and C. M. Soukoulis, Photonics Nanostruct. Fundam. Appl. **4**, 123 (2006).
[11]D. R. Fredkin and A. Ron, Appl. Phys. Lett. **81**, 1753 (2002).
[12]P. B. Johnson and R. W. Christy, Phys. Rev. B **6**, 4370 (1972).
[13]P. A. Belov and C. R. Simovski, Phys. Rev. E **72**, 026615 (2005).
[14]D. E. Aspnes, Am. J. Phys. **50**, 704 (1982).
[15]A. Taflove and S. C. Hagness, *Computational Electrodynamics-The finite Difference Time-Domain Method* (Artech, Boston, 2000).